Acta Cryst. (1959). **12**, 483

Complex Alloy Structures Regarded as Sphere Packings. II. Analysis and Classification of Representative Structures

By F. C. Frank
H. H. Wills Physical Laboratory, University of Bristol,

and J. S. Kasper
Research Laboratory, General Electric Company, Schenectady, New York, U.S.A.

(*Received* 29 *September* 1958)

The general principles and properties which have been deduced previously (Frank & Kasper, 1958) for the class of alloy structures with triangulated coordination polyhedra are applied in an analysis and classification of representative structures. In the main the analysis is with regard to the nature of layers and how they may be stacked and with regard to the nature of the major skeletons. Many hypothetical structures resulting from the analysis are listed and procedures are given for predicting other structure types. The relationship between alloy structures and inert gas hydrates is discussed.

1. Introduction

In Part I (Frank & Kasper, 1958) we have considered in a general sense complex alloy structures that are characterized by triangulated coordination shells. Topological and geometrical properties of such shells were discussed and justification was given for the prominence of four of them (with $Z = 12$, 14, 15 and 16) in actual structures. Also, the principles governing the combination of these shells into complete structures were deduced. In particular, two features of this class of structures were stressed—the existence of a major skeleton and the planar or approximately planar layering of atoms. We now undertake an analysis and classification of individual structures in terms of these two features utilizing the general properties and the terminology which have been discussed and defined in Part I.

2. Layering in triangulated shell structures

The familiar crystal structures based on the close-packing of equal spheres (the infinite series of structures of which f.c.c.* and h.c.p.† are the first two members) are often profitably regarded as assembled from layers all of which have the same triangular net pattern which is the closest packing of spheres in two dimensions. In this case there is a double choice in the stacking of each layer on the next. The choices may be designated $\triangle$ and ∇ and any repeating sequence of $\triangle$'s and ∇'s defines a member of this series of structures. These stackings generate just two kinds of coordination shell—the two non-triangulated 12-coordination shells.

In analogy with this, it is profitable to consider what kinds of layers there are which will stack together to form the structures with triangulated coordination shells. We have already demonstrated in Part I that layering is to be expected for these structures and that the primary layers (those in which atoms are in contact) are tessellations of hexagons, pentagons and triangles. It turns out, however, that only a small number of regular and semi-regular tessellations, together with certain systematic modifications of these, comprise the layer patterns for a large majority of the triangulated shell structures. Thus, the analysis in terms of layers is quite valuable.

2·1. *Layers with trigonal symmetry*

In trigonal symmetry the familiar structures utilize the two regular tessellations of this symmetry, 3^6 and 6^3 and just one of the semi-regular tessellations, 3.6.3.6 (Fig. 1). The numerical symbols used here are Schläfli symbols (Cundy & Rollett, 1954), specifying the number and sequence of various regular polygons around each vertex. The first is the triangular net—its vertices are in two-dimensional close packing. The second is the hexagonal or honeycomb net—a layer of graphite. The third corresponds to the three-way bamboo weave known as *kagomé*—a net of triangles and hexagons. This is a most important net of very wide-spread occurrence in crystal structures.

There are other semi-regular tessellations of 6-fold symmetry namely the two enantiomorphs of $3^4.6$; 3.4.6.4; 3.12^3; and 4.6.12. The dodecagon rings in the last two appear to make them unsuitable layers for structures with only moderate sized coordination shells. In all of these five cases the two-dimensional unit cell is large, so that if they occur at all it will

---

* Face-centered cubic.
† Hexagonal close-packed.

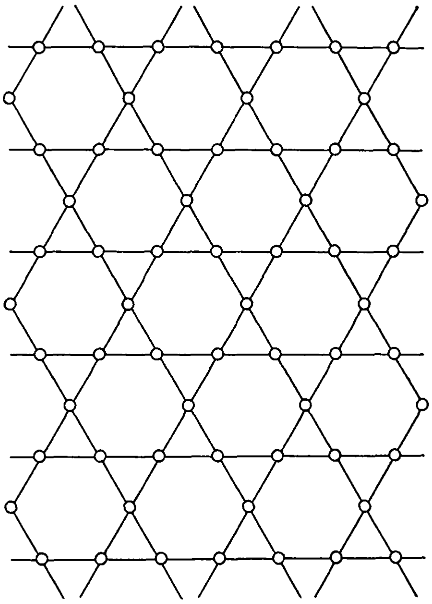

Fig. 1. Kagomé net 3.6.3.6.

only be in structures with a very large number of atoms per unit cell. There are, however, nets derived from these which can be used to construct structures of the type we are considering. An example of such a net, suggested by 3.4.6.4, is given in 2.5 and Fig. 16.

The simplest, and probably the commonest, of the kinds of structures which we are discussing is the class of closely related structures of composition AB_2 known as 'Laves phases'. We take (Fig. 2) (1) a kagomé net of atoms B', and stack on it (2) a triangular net of atoms A', centering its hexagons, then (3) a triangular net of atoms B'', centering half of its triangles (those in orientation △, let us say) followed (4) by a third triangular net of atoms A'', centering the remaining half of the kagomé triangles (those in orientation ▽). Another kagomé layer B''' stacked on to this pile, with its ▽ triangles over the B'' atoms and, therefore, over the △ triangles of the first kagomé net, makes a sandwich which is centrosymmetric with respect to the B'' atoms.

With regard to measurements, let the distance between nearest neighbors in the kagomé net be taken as 1. The distance between equivalent points in this net, and between atoms in each of the triangular nets is 2. The interplanar distance from kagomé to kagomé is $\sqrt{(8/3)}$, and the three triangular nets are respectively at 3/8, 4/8 and 5/8 of the distance between these planes. Thus, collectively, these triangular nets make a single puckered close-packed sheet of atoms, sandwiched between kagomé sheets.

The second kagomé net may be taken as the commencement of a similar sequence, or of an alternative sequence in which the B'' layer is placed to centre the triangles of ▽ orientation in the kagomé net below it (and the symbols △ and ▽ are correspondingly interchanged throughout the description).

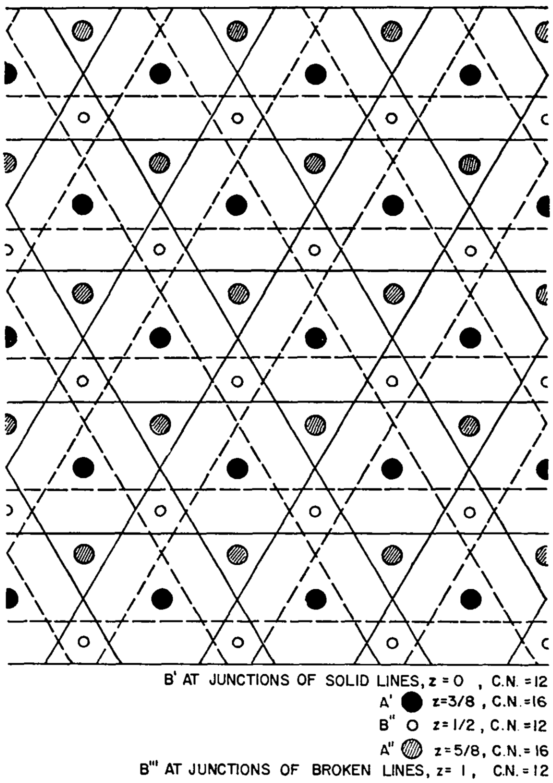

Fig. 2. In-filling of kagomé nets (at $Z = 0$ and $Z = 1$) in staggered superposition, as observed in Laves phases.

If the stacking first described, from kagomé to kagomé, is called △, and the alternative stacking ▽, then a variety of similar structures are described by various sequences of △ and ▽.

The sequence of repeating △ stackings makes a structure of cubic symmetry, with kagomé nets in all four (111) orientations. Repeated ▽ makes the same structure in twin orientation. This is the cubic Laves phase C_{15}, typified by $MgCu_2$. The sequence △▽, repeating, makes the hexagonal structure C_{14}, typified by $MgZn_2$. The sequence △△▽▽ makes the hexagonal structure C_{36}, typified by $MgNi_2$. These are the three "Laves phases". Other sequences are likely to be described as faulted versions of the other three. Their symmetry properties are defined by the △▽ sequence in just the same way as for the simple sphere-packing structures (Zhdanov, 1945; Frank, 1951).

The measurements given above are idealized ones, from which there are small departures except in the case of the cubic structure. With these measurements every B' atom has $6B$ atoms at distance 1 and $6A$ atoms at distance $\sqrt{(11/8)} = 1{\cdot}173$, making an icosahedral 12-coordination shell. Every A atom has $12B$ neighbors at $\sqrt{(11/8)}$ and $4A$ neighbors at $\sqrt{(3/2)} = 1{\cdot}225$ making the triangulated 16-coordination shell. These coordination numbers are independent of the

△▽ sequence, but the particular arrangement of A and B atoms in the icosahedral shells around the B' atoms (those in a kagomé layer) is different for the △△ and △▽ cases.

The structures just described have further crystallographic importance in representing the arrangement of cations in the spinel structure. They have the property that they can interpenetrate with a simple sphere-packing lattice made of triangular nets of C atoms, with interatomic distance 1, stacked at levels 2/8 and 6/8 of the distance between kagomé planes. In a △ stack as described above, one third of the atoms of the first C layer centres the ▽ triangles of the first kagomé plane. The second centres its △ triangles. Each △ stack of cations is associated with a ▽▽ stack of C atoms (oxygen ions). Then the A atoms fall in tetrahedral interstices and the B atoms fall in octahedral interstices of the close-packing of C atoms.

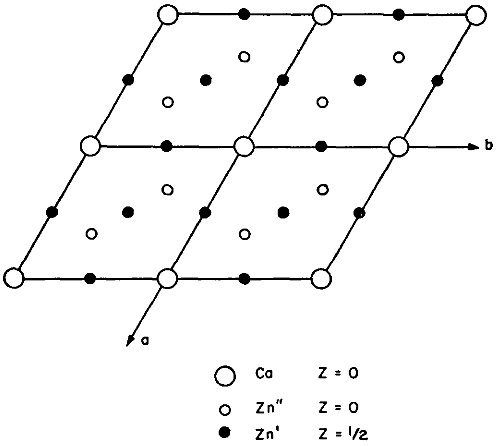

Fig. 3. The structure of $CaZn_5$.

In the structure of $CaZn_5$ (Fig. 3) there are just two alternate layers, a kagomé net of Zn′ atoms, with unit distance between neighbors, and a triangular net of Zn″ and Ca atoms, $\sqrt{(4/3)}$ between neighbors. Ca ions centre the kagomé hexagons and have a triangulated coordination shell of 18 Zn and 2 Ca atoms. One Zn atom, Zn′, has an icosahedral coordination shell of 8 Zn and 4 Ca. The other Zn atom, Zn″, has a novel kind of 12-fold coordination with 3 Ca and 9 Zn. The shell is triangulated but contains $3S_4$ as well as $3S_6$ and $6S_5$ surface coordinations.

A conceivable structure (Fig. 4), not known in isolation, could be derived from the previous one by splitting the Ca atom, with 20-fold coordination, into a pair of smaller atoms lying symmetrically on the hexagonal axis, each of which would have a somewhat asymmetrical triangulated 14-coordination shell. The coordination number of Zn″ atoms would then be raised from 12 to 15 (the normal triangulated shell for $Z = 15$).

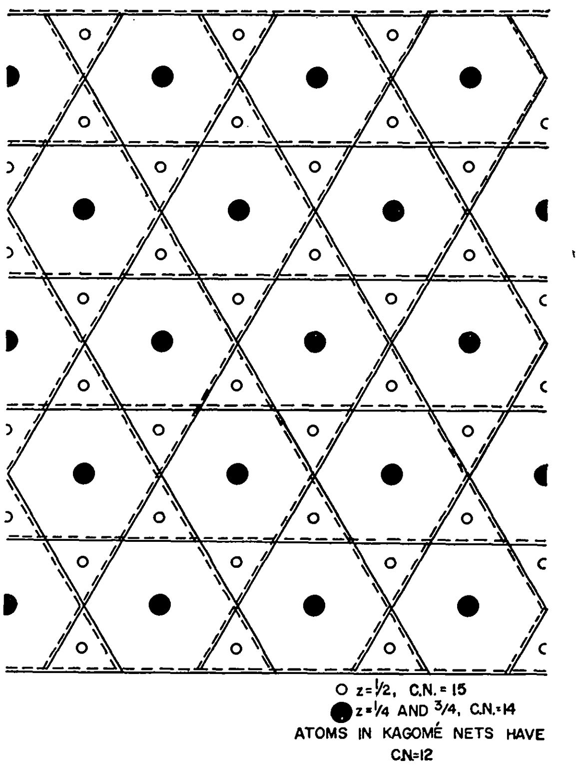

Fig. 4. In-filling of kagomé nets (at $Z = 0$ and $Z = 1$) in direct superposition, as observed in μ-phase.

This structure, though unknown in isolation, occurs in the μ-phase (e.g. Fe_7W_6, $D8_5$), which can be succinctly described as a succession of kagomé planes, with the interspaces alternately filled as in a Laves phase and as in our hypothetical 'split calcium $CaZn_5$ structure'. The coordinations undergo no change and the structure, therefore, has 12-, 14-, 15- and 16-coordination shells, all triangulated. There is a conceivable extensive family of structures of this kind. A suitable short notation to describe it is obtained by using the symbols △ and ▽ for the Laves-type kagomé stacking (accompanied by Laves-type in-filling of the space between them) in combination with 0 for a direct superposition of kagomé layers (with 'split calcium $CaZn_5$' in-filling). In this notation △0, repeating, defines the μ-phase and any other sequence of symbols △, ▽ and 0 defines a conceivable structure. The proportion of 14- and 15-coordination shells in the structures rises with the proportion of 0-stackings, relative to △ and ▽ stackings incorporated. A list of all possible structures up to 6 kagomé layers per repeat unit is given in Table 1. Only the one known example, μ phase, is given for a 6 layer repeat. It should be apparent how the table could be extended to any desired extent.

A further conceivable variation is that a proportion of particularly large atoms, with 20-coordination shells, can be incorporated in place of pairs of 14-coordinated atoms, by local reversion to the normal $CaZn_5$ structure. Examples of this are provided by ThM_5, Th_2M_{17}, where M = Fe, Co, or Ni and $ThMn_{12}$

Table 1. *Classification of triangulated shell alloy structures with three-fold symmetry*

Kagomé layers per repeat unit	Formula	Designation	Example	Layer sequence	Space group	No. of atoms in unit cell	Distribution of atoms for different Z				
							12	14	15	16	Average Z
1	A_4B_3	'Split $CaZn_5$'	—	0	$P6/mmm$	7	3	2	2	0	13·4
2	AB_2	Laves phase C_{14}	$MgZn_2$	△▽	$P6_3/mmc$	12	8	0	0	4	13·3
3	AB_2	Laves phase C_{15}	$MgCu_2$	|△|	$Fd3m$	24	16	0	0	8	13·3
	A_8B_{11}	(Hypothetical)	—	△0▽	$P3m1$	19	11	2	2	4	13·4
4	AB_2	Laves phase C_{36}	$MgNi_2$	△△▽▽	$P6_3/mmc$	24	16	0	0	8	13·3
	A_2B_3	(Hypothetical)	—	△△△0	—	25	15	2	2	6	13·4
	A_6B_7	(Hypothetical)	—	△▽00	—	26	14	4	4	4	13·2
	A_6B_7	(Hypothetical)	—	△0▽0	—	26	14	4	4	4	13·2
5	AB_2	(Hypothetical)	—	△△△△▽	$P\bar{3}m1$	30	20	0	0	10	13·3
	$A_{12}B_{19}$	(Hypothetical)	—	△△▽▽0	—	31	19	2	2	8	13·4
	$A_{12}B_{19}$	(Hypothetical)	—	△△▽0▽	—	31	19	2	2	8	13·4
	A_7B_9	(Hypothetical)	—	△△△00	—	32	18	4	4	6	13·4
	A_7B_9	(Hypothetical)	—	△0△0△	—	32	18	4	4	6	13·4
	$A_{16}B_{17}$	(Hypothetical)	—	△▽000	—	33	17	6	6	4	13·5
	$A_{16}B_{17}$	(Hypothetical)	—	△0▽00	—	33	17	6	6	4	13·5
6	A_6B_7	μ-phase	Fe_7W_6	|△0|	$R\bar{3}m$	13	7	2	2	2	13·2

(Florio *et al.*, 1956). ThM_5 is isostructural with $CaZn_5$; Th_2M_{17} is derived from ThM_5 by replacing in a regular manner one Th atom out of three by a pair of smaller M atoms; and $ThMn_{12}$ by replacing one Th out of two, in a hypothetical $ThMn_5$, structure, by a pair of Mn atoms. The structure of $BaMg_9$ (Goldish & Marsh, 1955) provides another illustration of partial replacement of large 20-coordinated atoms (in this case, Ba) by pairs of smaller 14-coordinated atoms (Mg atoms). The extent of this replacement is 40% for $BaMg_9$. These examples would suggest the possibility of structures with even higher extents of substitution of pairs of atoms for the large 20-coordinated atom and perhaps the attainability of the structure, designated 0, where this kind of substitution is complete.

2·2. *The case of 4-fold symmetry*

In four-fold symmetry we have one regular tessellation, the simple square net, and one important semiregular tessellation, the square-triangle net $3^2.4.3.4$, shown in Fig. 5. This net provides the closest packing of equal spheres in a plane in which there is 4-fold symmetry and every sphere has the same environment apart from orientation. Each has 5 equidistant neighbors.

When this net is rotated 90° about a 2-fold axis, the centres of squares coincide, and the overlapping squares are approximately in antisymmetric position (actually rotated 30° instead of 45°). A sequence of square-triangle layers (of Al) in these two orientations with intervening simple square nets (of Cu), centering their squares, describes the tetragonal $CuAl_2$ ($C16$) structure. Each Cu atom has a triangulated 10-coordination shell (8 Al, 2 Cu) and each Al a triangulated 15-coordination shell (11 Al, 4 Cu).

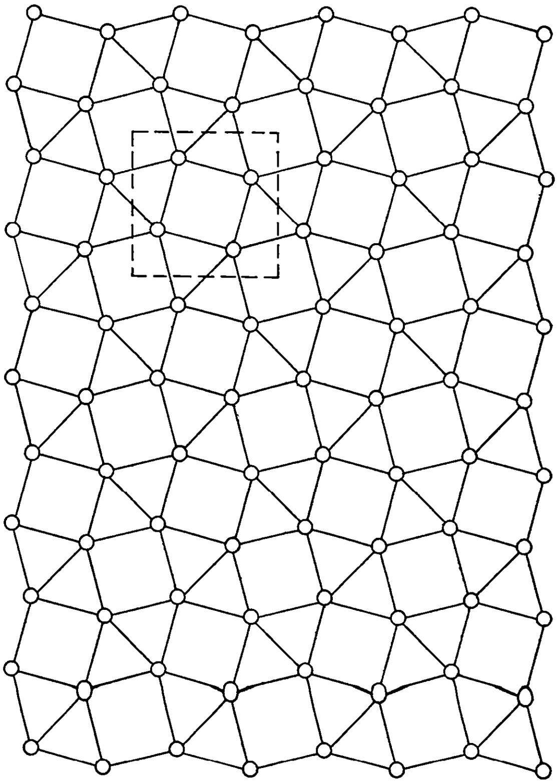

Fig. 5. $3^2.4.3.4$ net.

Another common structure with four-fold symmetry which we can utilize as a simple example of the way in which layer stacking produces higher coordination structures, is that of β-tungsten (A–15). We use the net (Fig. 6) with two kinds of vertex, two of $3^2.6^2$ to one of 3.6 3 6. If its hexagons are regular it has a rectangular unit cell with axial ratio $(1/2)\surd(3):1$. If the

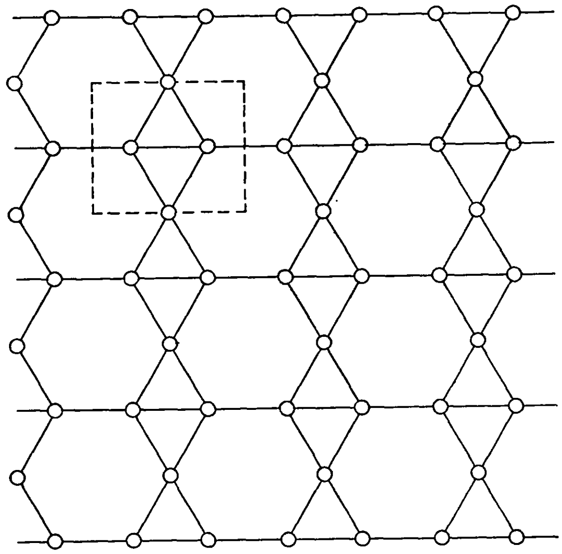

Fig. 6. The net for a layer in the β-W structure.

shorter axis is stretched to 1 to make the cell square, and the net is rotated 90° about one of its normal 2-fold rotation axes, in the centre of a hexagon, all the hexagon centres coincide. An alternate stacking of layers in these two orientations places hexagons antisymmetrically above each other, and at the same time places an atom approximately over the centre of each triangle. With these two layers at unit distance apart, a square net of atoms centering the hexagons, halfway between, completes the structure, which has cubic symmetry. Every atom possesses the best triangulated 14-coordination shell, though in somewhat distorted shape because of the prior deformation from regular hexagons which was required to square the unit cell of the net.

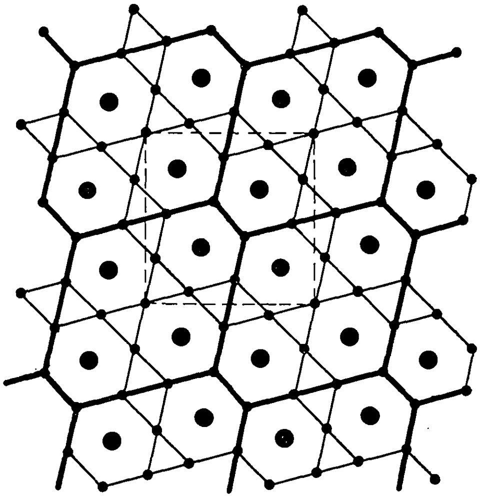

Fig. 7. Kagomé tiling.

There is a net of hexagons and triangles, possessing two-fold rotation-symmetry, which can be 'squared' with a much smaller distortion than in the foregoing case. This is shown in Fig. 7 and can be assembled from kagomé-patterned tiles having four hexagons and six triangles (outlined by heavy lines in Fig. 7). We shall call this important net 'kagomé-tiling'. (The same tiles can be assembled with two triangles each to make the true kagomé pattern.) The smallest unit cell of the kagomé-tiling net is rhombic, with diagonals in the ration $3\sqrt{(3)}:5 = 1{\cdot}04$. A shear of 4% makes it square. Either of two unit cells is a convenient one: one with its corners at the centres of four neighboring tiles, or one with its corners at the centres of short edges of tiles. After squaring the net, a rotation of 90° about the two-fold axis lying at the midpoint of a side of either cell (which is also the midpoint of a long edge of a 'tile') brings the one cell into superposition with the other. This operation superposes all the hexagons, essentially antisymmetrically. It also brings an atom approximately into the centre of each triangle. Two kagomé-tiling layers stacked above each other in this relationship fit very well together, and, like the simpler cases considered before, only require an interlayer of atoms centering the superposed hexagons to complete a well-coordinated structure. The pattern of this interlayer of 14-coordinated atoms is just the square-triangle net which was utilized in $CuAl_2$. The structure which results has tetragonal symmetry and is that of σ-phase, or of β-uranium.

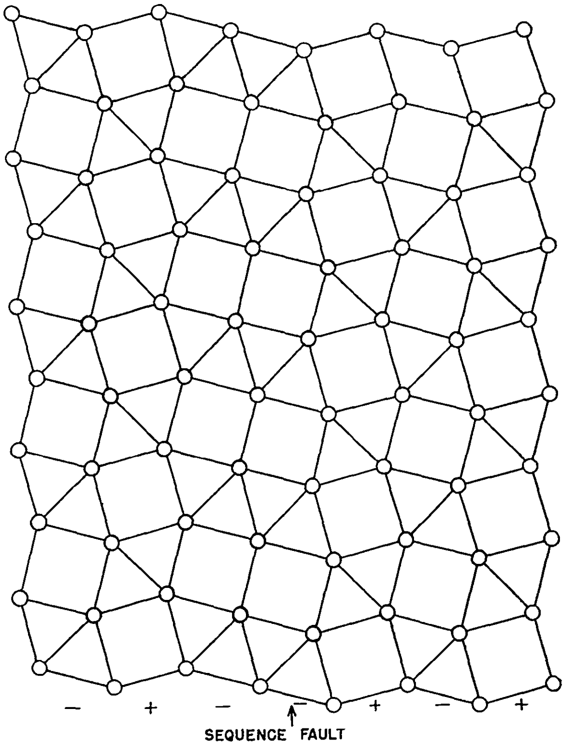

Fig. 8. A sequence fault in the $3^2.4.3.4$ pattern.

2·3. *Sequence faults in the σ-phase structure*

The square-triangle net (Fig. 5) may be seen as vertical zig-zag rows, cross-connected to each other in such a way that successive vertical zig-zags are alternately displaced up and down along their length relative to each other. Using + for up and − for down, the sequence of vertical zig-zag rows can be designated $|+\;-|$, repeating. Without changing the coordination numbers or neighbor–neighbor distances we may introduce a *sequence fault* into this pattern by having two successive + operations or two successive − operations in the sequence as in Fig. 8, representing the sequence $+ - + - - + - +$. One row of vertices is thus converted from $3^2.4.3.4$ to $3^3.4^2$. The same conversion performed throughout generates the semi-regular tessellation of two-fold symmetry which has all vertices of this type (Fig. 9). We should represent it by the sequence symbol $|+|$ (or $|-|$).

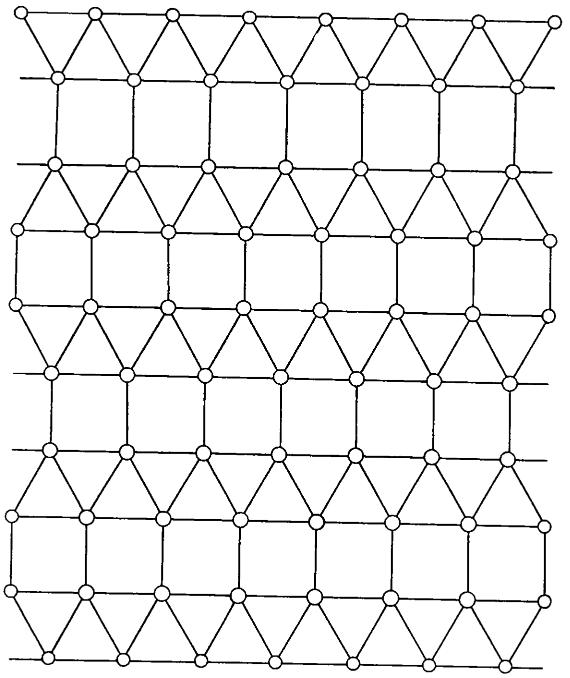

Fig. 9. $3^3.4^2$ tessellation.

It is a rather astonishing fact, which one would have had difficulty in foreseeing without guidance from the *P*-phase structure determined by Shoemaker, Shoemaker & Wilson (1957) that the kagomé-tiling pattern also allows sequence faults with which it continues to fit together in good coordination with the faulted square-triangle net.

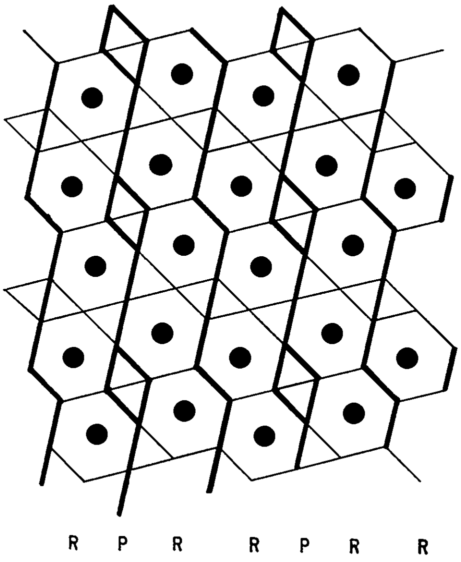

Fig. 10. Dissection of kagomé tiling into hexagon strips right-handed.

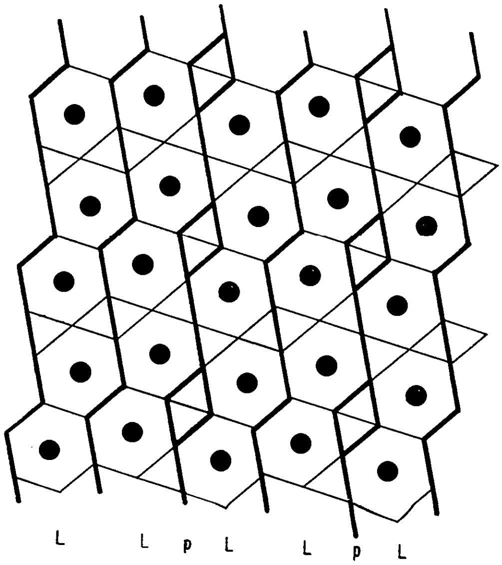

Fig. 11. Dissection of kagomé tiling into hexagon strips left-handed.

In order to describe these faults we first make an imaginary dissection of the un-faulted kagomé-tiling net into strips each of which contains the hexagons centered on a vertical zig-zag row of the square-triangle net. These are indicated by heavy lines in Fig. 10, which mark off staggered strips of hexagons and triangles which we shall call *right-handed hexagon-triangle strips* and denote by the letter *R*. Between every second pair of strips there is a line of triangle-pairs which we shall denote by the letter *p*. The relationship between centres is − when there is no interposed *p*-line and + when there is one. Fig. 11 shows the next overlying kagomé-tiling layer, similarly dissected. The difference is that the hexagon-triangle strips are left-handed. We designate them by the letter *L*. The relationship between centres is + when there is no interposed *p*-line, and − when there is one. Fig. 12 shows these layers superposed, in the

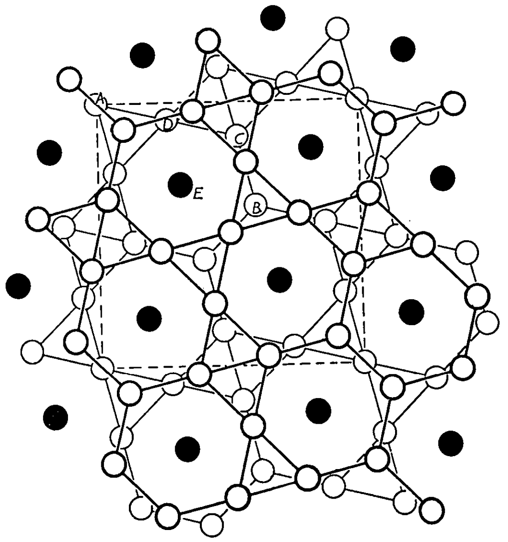

Fig. 12. The sigma phase structure.

normal σ-phase structure. Coordination requirements leave no choice in the relationship between strips. To provide an antisymmetric superposition of hexagons, L-strips must lie over R-strips, and conversely. Since the centre relationship in the succession LL is $+$, and that for RR is $-$, while an interposed p reverses the sign, p must lie over no-p, and conversely. We can use the notation just defined to give a symbolic description of the σ-phase structure, with its layers analysed into strips, as follows:

$$\begin{array}{c|c|l} p & L\cdot Lp & L\cdot Lp \\ & + \;\; - & + \;\; - \\ & RpR\cdot & RpR\cdot\ . \end{array}$$

Fig. 13 shows a corresponding strip dissection of a layer of the P-phase structure. In addition to hexagon-triangle strips (L and R both occurring in the layer) it contains pentagon-triangle strips. These are of one type only but occur in upward and downward positions, which we designate U and D. Whereas hexagon-triangle strips are denoted L and R according as their shoulders face forward on the left or right, pentagon-triangle strips are denoted U or D according as their shoulders face forward in the upward or downward direction. There are again lines of triangle-pairs between every second pair of strips. The sequence is

$$\begin{array}{c|c|l} pU\cdot & RpD\cdot LpU\cdot & RpD \\ - \;\; - & + \;\; + \;\; - \;\; - & + \ \ . \end{array}$$

The centre relationship is $-$ when R follows U, or D follows R, and $+$ when L follows D or U follows L, and interposition of p reverses the signs. L after U, U after R, R after D and D after L, with or without interposed p, are impossible sequences, not conforming at the joins.

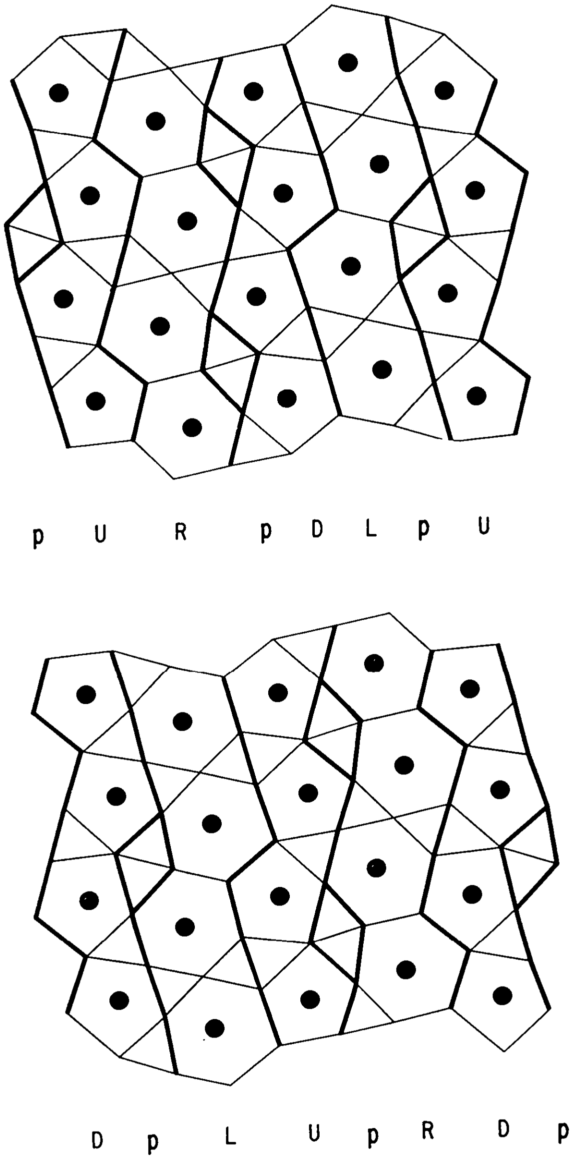

Fig. 13. Dissection of layers of P-phase into pentagon and hexagon strips.

Fig. 14 shows another layer stacked on top of this one to complete the P-phase structure. Coordination requirements uniquely determine its structure. For the pentagon-triangle strips we must have U over D or D over U for antisymmetric superposition of pentagons. We must have L over R and R over L for antisymmetric superposition of hexagons, as in σ-phase. Also as in σ-phase, we must have p over no-p, and no-p over p for conformity of $+$ or $-$ in the centre relationships. The symbolic designation of the complete P-phase structure is:

$$\begin{array}{c|c|l} \cdot Dp & L\cdot UpR\cdot Dp & L\cdot U \\ - \;\; - & + \;\; + \;\; - \;\; - & + \\ pU\cdot & RpD\cdot LpU\cdot & RpD\ . \end{array}$$

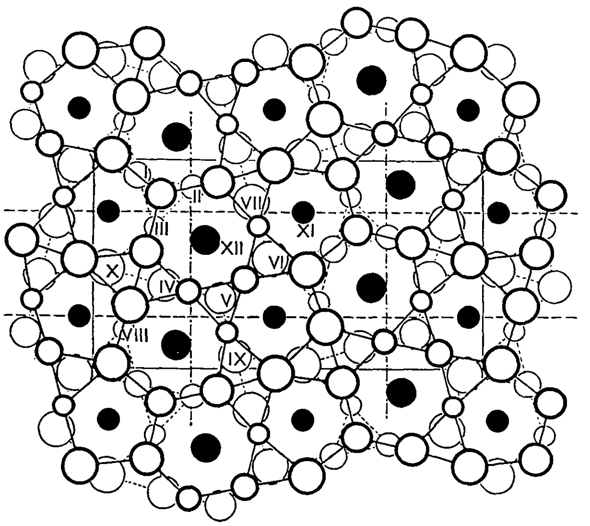

Fig. 14. The *P*-phase structure.

As a result of replacing hexagons by pentagons, we have now changed the coordination of a number of atoms from 14 to 12 (icosahedral). At the same time certain atoms (shown in the figure) acquire 16-coordination, again in best-triangulated form.

Though we have no example in a known crystal structure, there is no apparent geometrical objection to having two adjacent pentagon-triangle strips (with or without interposed *p*), provided that they are alternately *U* and *D*. The centre relationship will be + for *DU* and − for *UD*, with signs reversed when *p* is interposed. It is evident that this makes a satisfactory single layer, and one trial will suffice to verify that there is a satisfactory conformity in the stacking of layers. We shall make this trial after we have deduced the complete set of layer-structures permitted by the sequence rules derived above. To summarize these, the permitted sequences are:

LL, *LU*, *DL*, *DU*, all +;
RR, *RD*, *UR*, *UD*, all −;

and interposition of *p* interchanges + and −. The stacking rules *L* over *R*, *R* over *L*, *U* over *D*, *D* over *U* make the sequences conjugate to each other, as listed here, one pair or other having interposed *p*, to satisfy the further stacking rule + over +, − over −. The rule *p* over no-*p*, no-*p* over *p* is thus a necessary one. Thus we must have *LpL* above and below *R·R*, *L·U* above and below *RpD*, *LpU* above and below *R·D*, and so on. However, *L·L·U* above *RpRpD* would be an inadmissible stacking, since this would make strips of unequal width. The rule that *p* and no-*p* alternate in each sequence is, therefore, also a necessary one. With this rule it follows that:

+ + or − − sandwich either *U* or *D*
+ − or − + sandwich either *L* or *R* .

From these rules it follows that any chosen sequence of symbols + and − defines just two possible sequences of symbols *L*, *R*, *U*, *D*, *p*, which represent layers which are conjugate to each other in the sense that they must alternate in the stack. Hence, any chosen sequence of symbols + and − defines one and only one crystal structure in this general family.

A short designation of each member of the family is provided by a sequence of an even number of integers, representing alternately the number of successive + signs, and the number of successive − signs in a repeating unit of sequence.

Some early members of the infinite series of hypothetical well-coordinated structures so defined are set out symbolically in Table 2. The first structure (unknown) is illustrated in Fig. 15. It has as its interlayer, or secondary layer, the semi-regular tessellation $3^3.4^2$. This example provides the required verification that two successive pentagon-triangle strips do not produce an unforeseen difficulty in stacking. In this structure there are the four coordination polyhedra with $Z = 12$, 14, 15 and 16. All are in best triangulated form, with no severe distortions. The occurrence of two contiguous 16-coordinated atoms may be considered a demerit of the structure, but is also observed in *P*-phase. Since a coordination shell is always contained within one or two strips (together with the conjugate overlying strips), the illustrations of σ-phase, *P*-phase, and this structure, exhibit all the types of coordination that can occur in the whole family of structures. The composition of all members of the family, in terms of proportions of atoms with various coordination numbers, is intermediate between that of σ-phase and the structure of Fig. 15.

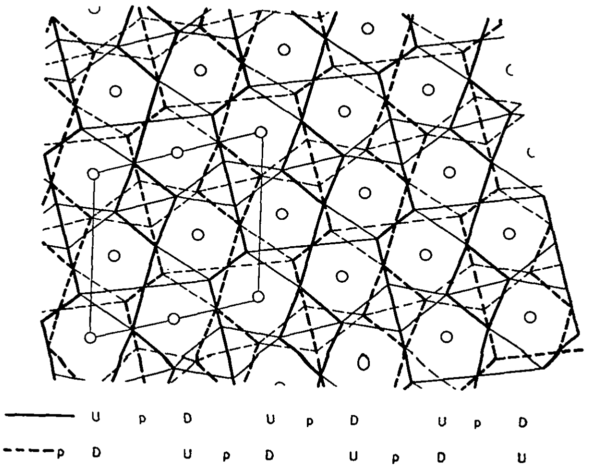

Fig. 15. Hypothetical structure containing only pentagon strips. (See note added in proof).

Each hexagon-pentagon-triangle plane is, from the stacking rules, a symmetry plane for the structure in which it lies. These structures are, therefore, in general monoclinic. A necessary condition for the symmetry

Table 2. *Structures based on $3^2.4.3.4$ tessellation and on sequence faults of that tessellation*

No. of sequences	Numerical symbols	Letter sequence	Name	Space group	Atoms per unit cell	No. of atoms for coordination of 12	14	15	16	Average Z
∞	∞	$\begin{vmatrix} UpD\cdot \\ +\ + \\ D\cdot Up \end{vmatrix}$	—	*Pm*	26	14	4	4	4	13·2
2	(1, 1)	$\begin{vmatrix} L\cdot Lp \\ +\ - \\ RpR\cdot \end{vmatrix}$	σ	*P*4/*mnm*	30	10	16	4	0	13·5
4	(2. 2)	$\begin{vmatrix} L\cdot UpR\cdot Dp \\ +\ +\ -\ - \\ RpD\cdot LpU\cdot \end{vmatrix}$	*P*	*Pbnm*	56	24	20	8	4	13·4
	(3, 1)	$\begin{vmatrix} L\cdot UpD\cdot Lp \\ +\ +\ +\ - \\ RpD\cdot UpR\cdot \end{vmatrix}$	—	*Pm*	56	24	20	8	4	13·4
6	(3, 3)	$\begin{vmatrix} L\cdot UpD\cdot LpU\cdot Dp \\ +\ +\ +\ -\ -\ - \\ RpD\cdot UpR\cdot DpU\cdot \end{vmatrix}$	—	*Pbnm*	82	38	24	12	8	13·4
	(4, 2)	$\begin{vmatrix} L\cdot UpD\cdot UpR\cdot Dp \\ +\ +\ +\ +\ -\ - \\ RpD\cdot UpD\cdot LpU\cdot \end{vmatrix}$	—	*Pm*	82	38	24	10	10	13·4
	(5, 1)	$\begin{vmatrix} L\cdot UpD\cdot UpD\cdot Lp \\ +\ +\ +\ +\ +\ - \\ RpD\cdot LpD\cdot UpR\cdot \end{vmatrix}$	—	*Pm*	82	38	24	10	10	13·4
	(3, 1, 1, 1)	$\begin{vmatrix} L\cdot UpD\cdot LpL\cdot Lp \\ +\ +\ +\ -\ +\ - \\ RpD\cdot UpR\cdot RpR\cdot \end{vmatrix}$	—	*Pm*	86	34	36	10	6	13·5
	(2, 1, 1, 2)	$\begin{vmatrix} L\cdot UpR\cdot RpR\cdot Dp\cdot \\ +\ +\ -\ +\ -\ - \\ RpD\cdot LpL\cdot LpU\cdot R \end{vmatrix}$	—	*P*1*nm*	86	34	36	12	4	13·4
	(2, 1, 2, 1)	$\begin{vmatrix} L\cdot UpR\cdot RpD\cdot Lp \\ +\ +\ -\ +\ +\ - \\ RpD\cdot LpL\cdot UpR\cdot \end{vmatrix}$	—	*Am*	86	34	36	12	4	13·4
8	(4, 4)	$\begin{vmatrix} L\cdot UpD\cdot UpR\cdot DpU\cdot Dp \\ +\ +\ +\ +\ -\ -\ -\ - \\ RpD\cdot UpD\cdot LpU\cdot DpU\cdot \end{vmatrix}$	—	*Pbnm*	108	52	28	14	14	13·4
	(121121)	$\begin{vmatrix} L\cdot UpR\cdot RpR\cdot DpL\cdot Lp \\ +\ +\ -\ +\ -\ -\ +\ - \\ RpD\cdot LpL\cdot LpU\cdot RpR \end{vmatrix}$	—	*Pbnm*	116	44	52	16	4	13·4

There are also 14 monoclinic structures for the 8 sequence group.

to be higher is that there are equal numbers of + and − signs in the repeating unit of the sequence. This condition suffices to ensure an essentially rectangular base for the unit cell, but two further conditions are needed to make the structure truly orthorhombic: (1) an antisymmetric sequence of + and − signs; (2) opposite signs occur at separations of 1/2 the repeating unit. Antisymmetry in the + and − sequence produces symmetry in the point array it represents, because the structure reflection across a plane normal to the sequence direction changes + into −. At the same time the associated letter sequences reflect into their conjugates. To prove this result, we note that from the sequence rules

(1) Reversal of signs in a + − sequence leaves the *L*, *R*, *U*, *D* symbols in the associated letter sequences unchanged, but transposes *p*.

(2) Reversal of direction in a + − sequence reverses direction in the associated letter sequences, and interchanges *U* and *D*, while

(3) A reflection of the structure, in a plane normal to the sequence direction, reverses direction and interchanges *L* and *R*, and

(4) Taking the conjugate layer interchanges *L* and *R*, *U* and *D*, and transposes *p*.

Hence operations (1) and (2) together, or (3) and (4) together, both have the same effect, reversing direction, interchanging *U* and *D* and transposing *p*. It follows that an antisymmetry in the + − sequence generates a glide-reflection plane normal to the basal symmetry plane and to the sequence direction. A second glide plane, parallel to the sequence direction, results if the antisymmetric sign sequence is such that opposite signs always occur at separations of 1/2 the repeat unit. For this plane, as for the one perpendicular to the sequence direction, a structure reflection changes + into −. With all these three elements of symmetry, the structure in general is orthorhombic with space group *Pbnm*. The first two examples of this in the general family are (1, 1) (σ-phase, actually tetragonal; the only member of the family which can have this symmetry) and (2, 2) (*P*-phase, orthorhombic). The next orthorhombic members in ascending complexity are (3, 3) and (4, 4) and (211, 211). The fact that the unknown early members of the family are of relatively low symmetry, coupled with the large numbers of atoms per unit cell implies that these structures could well exist without having yet been identified.

2·4. *Structures with sequence faults—general*

In the previous section, we have limited the discussion to those structures that contain primary layers of only one kind, the layers alternating in their orientation, to superimpose hexagons and pentagons antisymmetrically. It is possible, however, to use two different kinds of layers, alternately, to achieve satisfactory triangulated-shell structures, generally of low symmetry. Some of these structures may be obtained by the methods of the previous section with a slight modification of the rules. We still utilize hexagon and pentagon strips, lines of triangle pairs (*p*) and the same series of sequence faults designated by + and − signs. The strips are now no longer required to be of equal width and the previous rule that *p* and no-*p* alternate in each sequence does not apply. The number of allowed structures then becomes extremely large for even a small number of + − sequences. We give in Table 3 examples of those possible structures where the strips are all of one kind, either of hexagons or o

Table 3. *Faulted sequence structures*

Only hexagon strips in layers and unequal widths of strips. All of space group *P*2

No. of sequences	Numerical symbol	Letter sequence	No. of atoms in unit cell	No. of atoms for coordination of			
				12	14	15	16
∞	∞	*L*· + *Rp*	15	5	8	2	0
3	(2, 1)	*L*·*L*·*Lp* + + − *RpRpR*·	45	15	24	6	0
4	(2, 2)	*L*·*L*·*LpLp* + + − − *RpRpR*·*R*·	60	20	32	8	0
	(3, 1)	*L*·*L*·*L*·*Lp* + + + − *RpRpRpR*·	60	20	32	8	0
5	(4, 1)	*L*·*L*·*L*·*L*·*Lp* + + + + − *RpRpRpRpR*·	75	25	40	10	0
	(3, 2)	*L*·*L*·*L*·*LpLp* + + + − − *RpRpRpR*·*R*·	75	25	40	10	0
	(2, 1, 1, 1)	*L*·*L*·*LpL*·*Lp* + + − + − *RpRpR*·*RpR*·	75	25	40	10	0
		Pentagon strips only.	Space group *P*2				
2	(1, 1)	*UpDp* + − *D*·*U*·	26	14	4	4	4
4	(2, 2)	*UpD*·*U*·*Dp* + + − − *D*·*UpDpU*·	52	28	9	7	8
	(3, 1)	*D*·*UpD*·*U*· + + + − *UpD*·*UpDp*	52	28	9	7	8

pentagons alone. If both strips are allowed in one layer then an infinity of structures can be produced for a given numerical symbol.

In this group of structures the symmetry is lower and there is more variation from regularity in the coordination polyhedra than in the corresponding structures of the previous section. The existence of the two kinds of layers in μ-phase, however, does not permit these structures to be ruled out as possibilities, though they may be expected to be less likely to occur than the structures with only one kind of primary layer.

2·5. *Structures deducible from tiling patterns*

If two kinds of primary layers are permitted, it is possible to deduce many more structures than are suggested by the synthesis from hexagon and pentagon strips. We shall outline a general procedure, with only a few examples, for producing such structures.

First we take cognizance of the fact that a procedure exists for deducing the positions of atoms in neighboring layers from a given primary layer. This consists in placing atoms above the centers of triangles and above the centers of edges that are shared by hexagons or pentagons. Utilizing only hexagons and triangles we can then proceed to consider various nets that may be produced by a variety of tiling patterns, each of them being a portion of the kagomé net. Thus, a satisfactory tile can always be made by selecting a strip one hexagon wide from the kagomé net, the length being any desired number of hexagons provided we terminate the strips with the edges of hexagons. The simplest case is with one hexagon as the tiling unit itself. Placing atoms for the next layer above the centers of edges we obtain a kagomé net for that layer and the resulting structure is 'the split $CaZn_5$' structure that we have already considered. For two hexagons in a strip we also encounter a structure we have already deduced, in the previous section, with the formulation $\begin{vmatrix} L\cdot \\ + \\ Rp \end{vmatrix}$. With three or more hexagons per strip we obtain new structures, except when the length of strip is infinite. In that case, with a shear of 13% the net can be made square and the structure produced is that of β-W. All these structures, except that with infinite strip length, contain coordinations of 12, 14 and 15. No 15 coordination occurs in the β-W structure. The number of atoms with the different coordinations is easily deduced from the numbers of hexagons in a strip. If n is the number of hexagons per strip, then the number of atoms with $Z = 12$ is $3+2(n-1)$, the number with $Z = 14$ is $2+6(n-1)$, and the number with $Z = 15$ is 2 for all finite n.

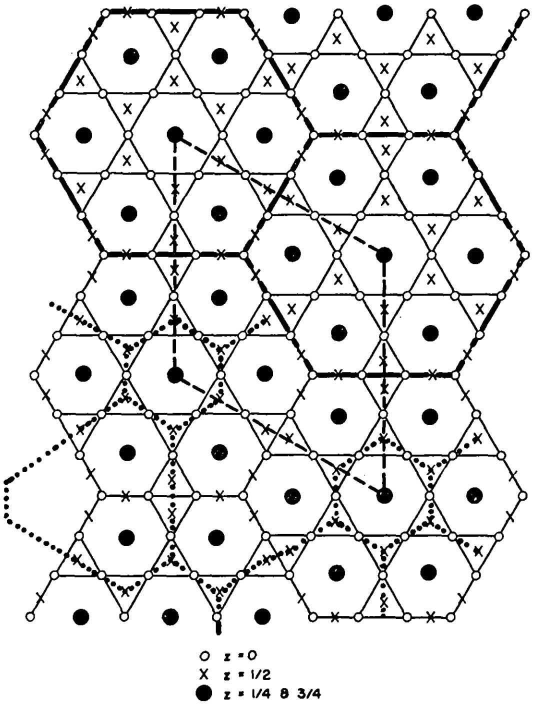

Fig. 16. Hypothetical structure based on large hexagon tiling unit. The borders of the tiling units are indicated by heavy lines, solid lines for the layer at $z = 0$, and dotted lines for the layer at $z = \frac{1}{2}$; the top part of the figure shows the former and the bottom part the latter.

There are other unit tiles that may be selected from the kagomé net to produce satisfactory hexagon-triangle nets from which triangulated shell structures could be made. We have already considered the tiling which contains four hexagons and which occurs in the sigma phase. We shall select only one additional example, shown in Fig. 16, where seven hexagons are contained in one tile which itself is a hexagon. The structure resulting from building the next layer and

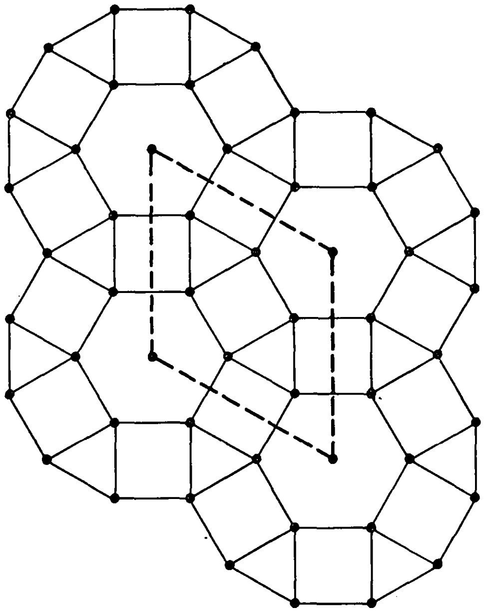

Fig. 17. A secondary layer for the hypothetical structure of Fig. 16.

centering the hexagons by major atoms is hexagonal and contains 52 atoms in the unit cell with the following distribution of coordination numbers: 18 of $Z12$, 26 of $Z14$ and 8 of $Z15$. In Fig. 17 we show the net for the secondary layer which may be viewed as derived from the semi-regular tessellation 3.4.6.4 except that each hexagon includes a point in its center. No examples of this structure are known.

2·6. *Secondary layers*

We have concentrated our attention on primary layers since they consist of atoms in contact and are most informative for an appreciation of the complete structure. We have noted in several instances, however, the simplicity and regularity of the pattern in the secondary layers and it is worthwhile to give some systematic consideration to these layers because they offer a means of simple classification of all the various structure types.

It appears in all cases we have treated that the secondary layers consist of triangles and squares (or rectangles that are almost square). This result is to be expected for triangulated shell structures from the considerations we have already given in Part I leading to the conclusion that layering, both primary and secondary, is a consequence for such structures. Reference to Figs. 4 and 5 of Part I should demonstrate the additional point not expressed there that the atoms in a secondary layer are arranged in triangles or squares (or slightly distorted squares) as a consequence of dealing with triangulated coordination shells.

It would seem a systematic general approach to deduce the possible tessellations of triangles and squares and from these proceed to the primary layers by centering hexagons, pentagons and triangles about the points in the secondary layer. These possibilities are too numerous, however, to be explored in detail. Furthermore, one secondary layer can be oriented in more than one way relative to another; it may superpose directly above another or it may be staggered. Accordingly, we shall forego complete generality, limiting our discussion to the simplest possibilities and to the actual secondary layers in the structures that have been observed or suggested by us. One simplifying feature, nonetheless, is that only one kind of secondary layer occurs in a given structure.

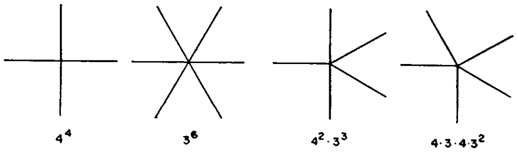

Fig. 18. The four kinds of points in nets constructed from square and triangle tessellations.

There are four kinds of points in a secondary layer, illustrated in Fig. 18. We may consider as the simplest situations the four nets wherein each point is equivalent. We find these correspond to examples we have already given. The 4^4 net is that for β-W, 3^6 nets occur in the Laves and μ-phases, $4^2.3^3$ applies to the hypothetical structure containing only pentagon strips in primary layers (Example 1, Table 2) and $4.3.4.3^2$ is the secondary net of σ-phase. It is difficult to decide on the order of simplicity in allowing combinations of two kinds of points in a net and we shall not pursue this point, but shall remark that our detailed exploration of the variations of σ-phase corresponds to finding combinations of $4^2.3^3$ and $4.3.4.3^2$ in the nets of secondary layers. Fig. 16 illustrates a combination of $4.3.4.3^2$ with 3^6 and the structure of $Mg_{32}(Al, Zn)_{49}$, discussed in section 4, is an example of the combination of $4^2.3^3$ with 3^6. It should be apparent how to proceed to synthesize other structures than those mentioned here starting from

Table 4. *Secondary layers in triangulated shell structures*

Structure	Nets	Comments
Laves phases	3^6	Different staggering sequence for C_{14} and C_{15}
μ-Phase	3^6	Nets of two kinds. In one net, triangles of same size as in Laves phases; in other, side of triangle is $\sqrt{3}/3$ of that in Laves phase
'Split $CaZn_5$ type'	3^6	Nets superposed directly over one another
β-W	4^4	Nets superposed directly above one another. Simple cubic lattice
σ-Phase	$4.3.4.3^2$	Nets superposed
P-Phase and other variations of σ-phase (except (1) Table 2) Tables 2 and 3	Combinations of $4.3.4.3^2$ and $4^2.3^3$	Nets superposed
Hypothetical pentagon-strip structure (1), Table 2	$4^2.3^3$	Nets superposed
$Mg_{32}(Al, Zn)_{49}$	Combinations of $4^2.3^3$ and 3^6	Nets staggered
Hypothetical structure, Fig. 17	Combinations of 3^6 and $4.3.4.3^2$	Nets superposed

an allowable secondary net. In this connection it must be pointed out that it is possible for the points in a secondary layer to center triangles of a primary layer, as well as pentagons and hexagons. This applies when the secondary nets are staggered, as in the Laves phases. If the nets occur directly superposed, then only pentagons and hexagons are to be centered about the points. In Table 4 there are listed in abbreviated fashion the kinds of nets in the secondary layers and how they are put together in the various structures.

3. The major skeletons

While the layering analysis of triangulated shell structures is perhaps the most informative as to details of structure, it is instructive and useful also to consider the major skeleton. Its relative simplicity and the ease of producing the full structure by inserting hexagons of atoms normal to all its bonds aids in remembering and reconstructing some of the more complex structures. We shall discuss the various structures in the same order as in the discussion of layering.

3·1. *Trigonal symmetry*

Laves phases.—For these the skeletons are especially simple. The cubic C_{15} structure has the diamond structure for its major skeleton. The hexagonal C_{14} structure has the corresponding hexagonal or twin variant of the diamond arrangement. Just as the C_{36} structure, typified by $MgNi_2$, is the simplest faulted arrangement involving the layer sequences of both C_{14} and C_{15}, its major skeleton is obtained by a corresponding alternation in the major skeletons of C_{14} and C_{15}. Similarly, the more highly faulted structures that may be postulated may be derived from the corresponding twinned major skeleton.

Hypothetical structure derived from $CaZn_5$.—The major skeleton is a simple one here, also. It consists of graphite-type sheets stacked directly over each other with strings of atoms threading each hexagon, normal to the sheets, a pair of atoms in a string ($Z = 14$) located midway between two sheets of atoms with $Z = 15$.

μ-Phase.—The major skeleton of μ-phase is compounded from the diamond structure and the skeletons of the split $CaZn_5$ structure, described above. Viewing the diamond structure with a trigonal axis vertical, insertion of a pair of atoms along each vertical bond and a graphite-like layer sandwiched by this pair produces the major skeleton of μ-phase. Z is 14 for the inserted pair of atoms, 16 for the other atoms to which they are joined, and 15 for those in the graphite-like sheets.

Variation of μ-phase.—There is no need for detailed description of the major skeletons of the numerous possible structures based on different $\triangle$, ∇ and 0 sequences as discussed in the section on layering and indicated in Table 1. They all are compounded from the skeletons of the Laves phase and the split $CaZn_5$ structure, the sequence and proportions being readily deducible from the layer symbolism of the structure.

3·2. *Four-fold symmetry*

A–15 or β-W structures.—For this simple structure the major skeleton contains the 6 atoms at $\pm(0, 1/2, 1/4; \curvearrowright)$ but with connections between atoms only along the three $\langle 100 \rangle$ directions. There result then three independent systems of major rows along the $\langle 100 \rangle$ directions, each row bisecting a (100) face, with atoms at 1/4 and 3/4 of a unit-cell translation.

σ-Phase structure.—The borders of the kagomé tiling pattern of Fig. 7 together with the row of atoms (4 per tile) normal to the plane represent the major skeleton of σ-phase. Atoms at the tile corners are 15-coordinated and those in tile edges and in the vertical rows are 14 coordinated. Alternate layers have the same kagomé tiling but are rotated 90° relative to one another. There is no connection between the layers in the structure of the skeleton.

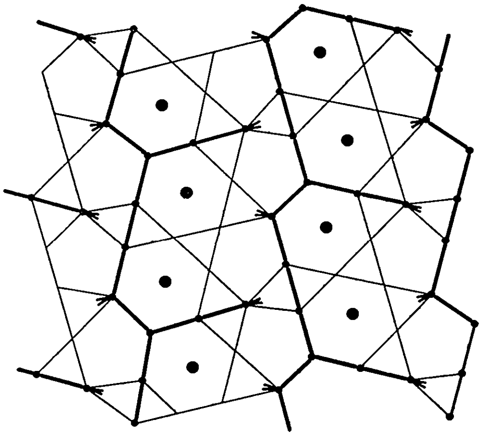

Fig. 19. The major skeleton of the P-phase structure.

P-phase and other structures that are related to σ-phase.—For P-phase and the numerous hypothetical structures that are related to σ-phase, the major skeleton is considerably more complex than for σ-phase, the complexity arising from the presence of pentagons in the primary layers. Thus, in none of these structures does there appear a tiling pattern within a primary layer as for σ-phase; rather, there are zig-zag rows with different degrees of branching, and with connections between successive primary layers. Fig. 19 illustrates the skeleton for P-phase, depicting the connections within one layer and showing by two unterminated lines the bonds to atoms in a layer above and below the illustrated one. Also, in all cases other than σ, the projected positions of atoms in the rows centering hexagons give rise to zig-zag rows wherever a hexagon strip occurs in the primary layer, rather than to simple tessellations.

In the simplest structure of this class, wherein the layers contain exclusively pentagons, the skeleton

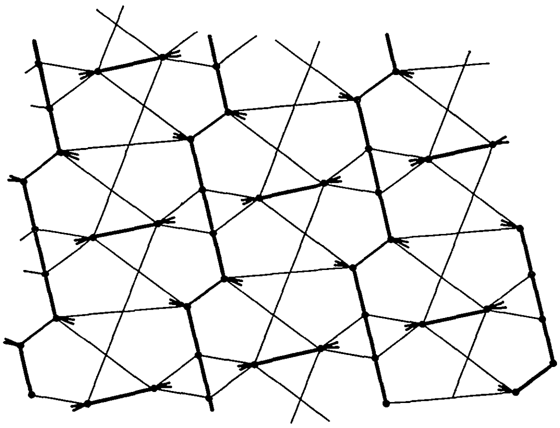

Fig. 20. The major skeleton of the hypothetical structure with pentagon strips only. (See note added in proof).

structure contains, of course, no rows of atoms normal to the layers and there is a maximum number of connections between layers. This is illustrated in Fig. 20, where again only one layer is shown, but bonds to atoms in adjacent layers are indicated by unterminated lines.

3·3. *Structures based on different tiling patterns*

The nature of the major skeletons here is considered in the general discussion in 3·4. The heavy lines in Fig. 16 outline the major skeleton of the hypothetical structure discussed in 2·5.

3·4. *The major skeleton in layered structures*

If a layer in a normally coordinated structure is a kagomé tiling, in the general sense that it may be dissected along ligands into areas of kagomé pattern, with a breach of the pattern at the dissections, then all the ligands along the dissection lines are major ligands. All other ligands are minor. This is readily established from the fact that ligands within a kagomé-patterned area are shared by a hexagon and a triangle in the plane, while those along the dissection lines are shared either by two hexagons or two triangles. Thus the tile borders make up the major skeleton lines within the layer. The only possible tiles are hexagons (not necessarily regular) with kagomé pattern hexagons in their corners. The other seeming possibilities (with included angles at the corner of 60°, 240° or 300°) are excluded either by making no breach in the kagomé pattern or making an impossible arrangement of major ligands (three in a plane, 60° apart). Every tile corner is the meeting point of three tiles, the corresponding atom being 15-coordinated. Atoms along the straight edges of a tile are 14-coordinated.

When the layer pattern contains pentagons, and is, therefore, not a kagomé-tiling pattern, the ligands shared by hexagons and pentagons (or by two pentagons) are major. The system of major ligands in the layer is now found to have single ended terminations, and corners which are not triple junctions, in addition to the connections characteristic of the tiling layers (see for example Fig. 19). The single ended terminations correspond to $Z15$ atoms with major ligands leading out of the plane, one on each side: the corners which are not junctions correspond to $Z16$ atoms, again with one major ligand leading out of the plane on each side of the layer. It follows that a non-tiling layer must be followed (after the appropriate secondary layer) by another non-tiling layer; and, conversely, that a tiling layer must be followed, after the secondary layer, by another tiling layer. In general, this will be a different tiling pattern from the first. In applying this rule it must be understood that a single hexagon of the kagomé pattern can count as a kagomé-patterned tile.

The foregoing identifies all parts of the major skeleton lying in the layer itself. In addition there are, of course, major ligands perpendicular to the layer, connecting secondary layer atoms, at the centre of every hexagon in the pattern.

4. The structure of $Mg_{32}(Al, Zn)_{49}$

Recently, the crystal structure of a phase with the formula $Mg_{32}(Al, Zn)_{49}$ has been determined by Bergman, Waugh & Pauling (1957). This structure is another example, probably the most complex one to be reported, of the class of structures under discussion. There occur the four well-triangulated coordination polyhedra in the following proportions: 98 with $Z = 12$ (icosahedral); 12 with $Z = 14$; 12 with $Z = 15$; and 40 with $Z = 16$. The average coordination number is 13·4.

Our analysis to this point does not lead us directly to the $Mg_{32}(Al, Zn)_{49}$ structure. On the other hand, according to our general principles, it should be possible to analyze this structure, too, in terms of primary hexagon-pentagon-triangle layers and a major skeleton and we shall demonstrate this. Nonetheless, this structure appears to be a special case. As described by the authors, it represents the result of maintaining icosahedral packing. Starting with an icosahedron, spheres are added in successive shells in a manner always to center the triangles of previous shells. A complex of 117 atoms can be built up, with 72 atoms in the outermost shell lying on the faces of a cuboctahedron. The cuboctahedra can then be packed in a body-centered cubic lattice, with a sharing of the 72 atoms between neighboring complexes, giving 162 atoms in a unit cube. In order to accomplish this arrangement there is a steady increase in the size of spheres for successive outer shells and it is found that the larger Mg atoms do occur in the outer shells.

Plane or approximately plane layers of hexagon-pentagon-triangle arrangements occur parallel to (001). Fig. 21 shows the plane layer at $z = 0$, with the

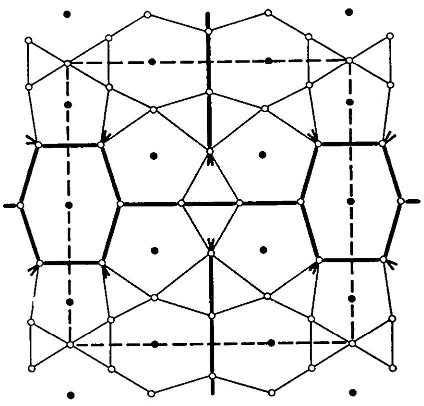

Fig. 21. The plane layer at $z = 0$ for the $\mathrm{Mg_{32}\,(Al, Zn)_{49}}$ structure.

positions at $\pm 0{\cdot}1$ (approximately) centering the hexagons and pentagons. It is a more complex arrangement than we have encountered in the other structures but a satisfactory one according to our rules for such layers. The same plane layer occurs at $z = 1/2$, but shifted by the body-centering translation. It is to be noted from Fig. 21 that the secondary layer of atoms at $z = 0{\cdot}1$ is a tessellation combining $4^2.3^2$ and 3^6 junctions.

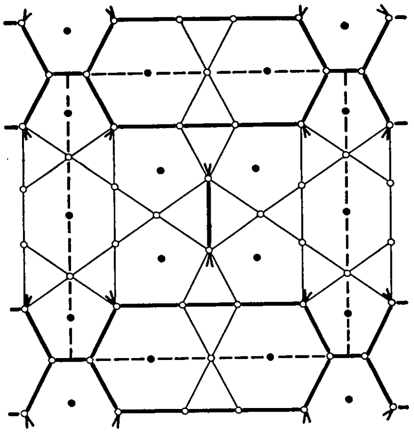

Fig. 22. The layer at $z = 0{\cdot}2$ in the $\mathrm{Mg_{32}(Al, Zn)_{49}}$ structure. Solid circles are at $z \pm 0{\cdot}1$.

At $z = 0{\cdot}2$ and $z = 0{\cdot}3$, approximately, the nearly plane layers are those shown in Fig. 22, the layer at $z = 0{\cdot}3$ being shifted by half a face diagonal translation relative to that of $z = 0{\cdot}2$. The same layers occur also at $z = 0{\cdot}7$ and $z = 0{\cdot}8$. The amount of puckering is generally small ($\pm 0{\cdot}03$ in z) but one kind of atom with $z = 0{\cdot}15$ needs to be considered as belonging to the layer at $z \pm 0{\cdot}2$. We encounter with this structure a modification of the principles of layering used so far. We have indicated that the plane layer at $z = 0$ is a satisfactory primary layer and leads to secondary layers at $\pm 0{\cdot}1$ approximately. Also, the puckered layers at $\pm 0{\cdot}2$ appear to be primary and can be derived from the layer at $z = 0$ by rule of centering the triangles and the edges shared by hexagons or pentagons. The same layer sequence, but with a translation of 1/2, 1/2, 0, occurs if we start with a plane layer at $z = 1/2$ and proceed to $z = 0{\cdot}4$ and $0{\cdot}6$ and $z = 0{\cdot}3$ and $z = 0{\cdot}7$. There seemingly results the juxtaposition of two primary layers at $z = 0{\cdot}2$ and $0{\cdot}3$, (also at $z = 0{\cdot}7$ and $0{\cdot}8$), with no intervening secondary layer. Nonetheless, because of the actual puckering of these layers, satisfactory triangulated coordinations are achieved, a situation that would not be realizable were the layers planar as in the cases considered up to this point.

This structure demonstrates how deviations from strict planarity of primary layers may occur but how the layer analysis still applies in a broad sense. It also indicates the difficulty of formulating all possible structures with triangulated shells, especially when deviations from planarity are allowed.

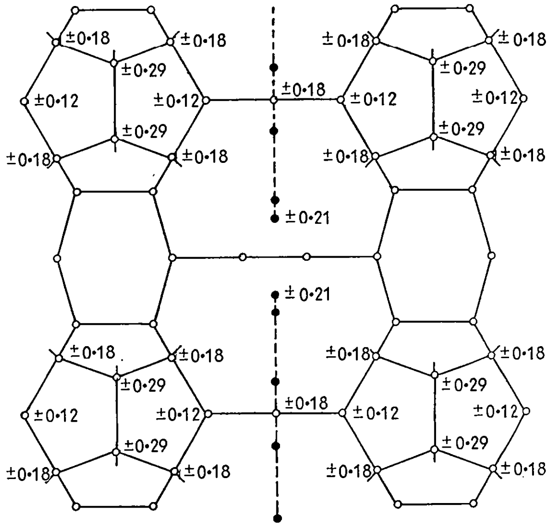

Fig. 23. The major skeleton of the $\mathrm{Mg_{32}(Al, Zn)_{49}}$ structure.

Major ligands in the principal layers have been indicated by heavy lines in Figs. 21 and 22. The three-dimensional major skeleton is indicated in Fig. 23. It consists only of magnesium atoms, and contains all 64 of these in the unit cell. The 16-coordinated atoms form pentagonal dodecahedra, in one orientation centered on the origin and in a second orientation around the body-centre. (There are 20 $Z16$ atoms in each.) Only one set of these are shown in Fig. 23. 6 edges of each dodecahedron link to edges of neighboring dodecahedra of the same set through pairs of 15-coordinated atoms, with which they make hexagons. These $Z15$ atoms are linked in pairs by pairs of $Z14$ atoms. There are thus 6 $Z15$ and 6 $Z14$ atoms per dodecahedron. The major ligand connecting the $Z14$ pair passes centrally through a hexagon associated with the second set of dodecahedra. (Shown with broken lines in Fig. 23.) There remain eight major ligands from each dodecahedron directed along ⟨111⟩ axes, by which it connects with neighboring dodecahedra of the second set. In this way the major skeleton is fully connected.

5. The α-manganese structure

There are some structures, most notably that of α-manganese, where some of the triangulated polyhedra for $Z = 12$, 14, 15, 16 occur along with other coordination polyhedra that are not triangulated. Thus, in α-manganese 24 of the 58 atoms per unit cell have icosahedral coordination, 10 have the triangulated $Z16$ coordination, but the remaining 24 have 13 neighbors forming a non-triangulated shell. Accordingly, this structure is not a member of the class of structures under discussion and our principles and generalizations do not apply to it. For example, the α-manganese structure cannot be dissected into plane or approximately plane hexagon-pentagon-triangle layers and ambiguity results in attempting to classify the 13-coordinated atom as major or minor. One of us (Kasper, 1956) has incorrectly assumed previously that it was permissible to regard the coordination for this atom as 14 by allowing an extra atom, at quite a distance from the central one, within the coordination shell. This is clearly not permissible by the rules (2·1, Part I) we have established for deducing the coordination shells. The true coordination for this atom is 13, and the α-manganese structure is not a representative of the class of fully triangulated coordination shell structures.

The major ligand concept can still be usefully applied. There is a normally coordinated $Z16$ atom at the origin, with 4 normally coordinated $Z16$ neighbors, connected in pairs through 6 pairs of abnormally coordinated atoms. This has the effect of isolating a small unit of diamond-like major skeleton. Such tetrahedral units occur in one orientation at the origin and reverse orientation at the body centre. The positions so singled out are those which Laves *et al.* (1934) suggested were occupied by Mg atoms in the isostructural alloy $Mg_{17}Al_{12}$.

6. The structures of inert gas hydrates

It is a fascinating matter that there exists a strict correspondence between the structures of such chemically different substances as the gas hydrates and the intermetallic compounds of the class we have considered here. Two cubic structures (Claussen, 1951; Pauling & Marsh, 1952; Stackelberg & Muller, 1951) have been reported for the gas hydrates. In one structure, the water molecules form two kinds of cages which enclose the gas molecule—a pentagonal dodecahedron and a 14-face polyhedron (tetrakaidecahedron) in the respective proportions of 1 to 3. The centers of these cages are located at the points of the A–15 or β-W structure. In the other gas hydrate structure there occurs again the pentagonal dodecahedron but the other cage is a 16-face polyhedron (hexakaidecahedron). Their proportions are 2 to 1 respectively and their centers are the positions of the cubic Laves or $C15$ structure. These polyhedra are in fact the duals of the icosahedron, the $Z = 14$ and $Z = 16$ triangulated shells we have dealt with in the alloy structures.

A convenient way of describing the hydrate structures then is in terms of the analogous metal structures by focusing attention on the positions of the centers of water cages (or the gas molecule positions). In one case, these positions are given strictly by the β-W structure. The water molecules are then centered in each of the tetrahedra of the β-W structure, 46 per unit cell, to give the complete hydrate structure with 46 water molecules, 2 smaller cages around the minor sites and 6 larger cages around the major sites. For the other structure we consider the $C15$ Laves structure, for which there are 16 minor sites, 8 major sites and 136 tetrahedra. We place a water molecule in the center of each tetrahedron and associate a gas molecule with the major and minor sites to produce the complete hydrate structure. The 16-face cage results around the major sites and the dodecahedron around the minor sites.

This relationship between the gas hydrate structures and those we have been considering is a logically natural one, since the sphere-packings with all triangulated coordination polyhedra are *ipso facto* those with all tetrahedral interstices, and further have the property that each tetrahedral interstice is tetrahedrally surrounded by four more, providing the right coordination of water-molecules for complete hydrogen-bonding. It is worth noting that whereas in the diamond-like ice structure obtainable by low temperature sublimation, the hydrogen bonds of neighboring molecules are always in *trans* configuration, in the ordinary hexagonal ice structure the configuration is *cis* for pairs along the hexad axis, and otherwise *trans*, the configuration is *cis* throughout for interstitial water molecules in any sphere-packing with all triangulated coordination. This follows immediately from the fact that adjacent tetrahedra of spheres share triangular faces.

Since the A-15 and C-15 structures are only two representatives of a very extensive class of metal structures, it is tempting to suggest possible hydrate structures that are related to other metal structures. In the absence of thermodynamic criteria, there is no reason to preclude hydrate structures that can be derived from the hexagonal Laves phase or C–14 structure. This would contain the same water cages and in the same proportions, leading to identical hydration numbers as for the established cubic hydrate structure with a_0 of 17 Å. More interesting would be hydrate structures derived from the complex metal structures, σ-phase and μ-phase, for example. It is noteworthy that the hydration number for small molecules (the total number of H_2O molecules divided by the total number of cages) would not vary significantly for all the possible postulated structures. For those derived from σ-phase and μ-phase, for instance, the hydration numbers (small molecules) would be 5·73 and 5·69. These numbers for the two established structures are 5·75 (12 Å cell) and 5·67 (17 Å cell). The hydration numbers for large molecules (number of H_2O molecules divided by number of large cages) would vary with structure type, of course; 8·6 for σ-phase and 12·3 for μ-phase.

7. General remarks

While we have treated many examples both of known and hypothetical structures, our treatment cannot be claimed to be all inclusive in either case. We believe, however, that our principles and analysis are applicable to any examples that may have been omitted or which will be found of structures wherein the 4 normal coordinations only occur. We feel it is quite likely that such examples will occur.

There are questions of a more physical nature which we have not considered. One such question is that concerning ordering, or more precisely the association of different component elements with the different coordinations in an alloy. In some instances, as in the Laves phases, the situation is clear and well-known. A significant size difference is required for the Laves phase structure and the A atom (for the formulation AB_2) is the larger atom in a two-component system. In other cases, as in the σ-phases, there are varying degrees of order according to the combinations of elements and no direct correlation with usual atom radii can be made.

A rule of fairly general validity is that the $Z14$ and $Z15$ sites (for which the coordination shells are respectively somewhat oblate and prolate, whereas $Z12$ and $Z16$ are more nearly spherical) are only occupied by transition metal atoms. The striking exception is magnesium.

The extent to which packing considerations in contrast to other factors are determinative in choice of structure cannot be readily ascertained. It is quite usual to attribute the determinative role to 'electronic factors' for σ-phase, for example. It is our position' however, that the packing considerations are of primary importance and that electronic factors may be operative in selecting between alternative structures that satisfy the packing requirements.

Note added in proof. — Mr. H. J. Beattie Jr. has recently pointed out to us an inaccuracy in our text. In section 2.3 we state that the structure containing only pentagon-triangle strips is unknown and we designate it as 'hypothetical' in Figures 15 and 20. In point of fact, this structure is essentially that of μ-phase, discussed in section 2.1. While the monoclinic description given in Table 2 (first entry) is correct in general, the most symmetrical topologically equivalent structure is rhombohedral (μ-phase). Accordingly, the major skeleton of Figure 20 may be seen to fit, topologically, the description of the μ-phase major skeleton given in section 3.1.

References

Bergman, G., Waugh, J. L. T. & Pauling, L. (1957). *Acta Cryst.* **10**, 254.

Claussen, W. F. (1951). *J. Chem. Phys.* **19**, 259, 1425.

Cundy, H. M. & Rollett, A. P. (1954). 'Mathematical Models'. Oxford: Clarendon Press.

Florio, J. V., Baenziger, N. C. & Rundle, R. E. (1956). *Acta Cryst.* **9**, 367.

Frank, F. C. (1951). *Phil. Mag.* **42**, 1014.

Frank, F. C. & Kasper, J. S. (1958). *Acta Cryst.* **11**, 184.

Goldish, E. & Marsh, R. E. (1955). Abstract of Meeting of American Crystallographic Association, June 27–July 2.

Kasper, J. S. (1956). 'Theory of Alloy Phases', ASM Symposium, p. 268.

Laves, F., Löhberg, K. & Rahlfs, P. (1934). *Nachr. Ges. Wiss. Göttingen, Math.-phys. Kl,* Neue Folge (1), **67**.

Pauling, L. & Marsh, R. E. (1952). *Proc. Nat. Acad. Sci. Wash.* **38**, 112.

Shoemaker, D. P., Shoemaker, C. B. & Wilson, F. C. (1957). *Acta Cryst.* **10**, 1.

Stackelberg, M. V. & Muller, H. R. (1951). *J. Chem. Phys.* **19**, 1319.

Zhdanov, C. S. (1945). *Comptes Rend. U.S.S.R. (Doklady)* **48**, 39.